CHAPTER 8

Investigation on the interactions stabilizing the $A\beta_{1-42}$ peptide oligomers and $A\beta_{1-42}$ fibril polymorphs

Investigation on the interactions stabilizing the $A\beta_{1-42}$ peptide oligomers and $A\beta_{1-42}$ fibril polymorphs

8.1. Abstract:

$A\beta_{1-42}$ peptide aggregation is known to be an important factor in the causation of AD. Smaller oligomers, the intermediates during the process of aggregation, are known to be more neurotoxic than matured fibrils. The structural dynamics of $A\beta_{1-42}$ peptide oligomers at atomistic level and the interactions holding the monomeric units in the oligomeric structures still remains elusive. In this study, we have investigated the structural dynamics of the toxic $A\beta_{1-42}$ peptide intermediates and analyzed the simulation trajectories to examine the interactions that stabilize the oligomers. From the structural dynamics of $A\beta_{1-42}$ peptide oligomers, we observed the significant number of secondary structural transitions from α-helix to random coils in some of the monomeric units. From the interaction study, we noticed the involvement of hydrophobic contacts and inter-molecular hydrogen bonds in stabilizing the oligomers. Additionally, we subjected the equilibrated structure of the oligomers in PDBsum server [180] to examine the protein-protein interactions. The interaction results obtained from the PDBsum server was found to be consistent with the results obtained from the trajectory analysis. It has been suggested that $A\beta_{1-42}$ oligomerization may occur through several mechanisms which can be confirmed from the availability of different $A\beta_{1-42}$ fibril polymorphs in the senile plaques. Therefore, we have examined the structural variations, and carried out interaction studies of the $A\beta_{1-42}$ fibril polymorphs reported in Protein Data Bank using the PDBsum server. From our study, we found the presence of turn and extended β-stranded secondary structure predominantly in the region 11-42 of $A\beta_{1-42}$ fibril in all the polymorphs. Furthermore, we found primarily the residues from CHC region and C-terminal region to be involved in the intermolecular interactions.

8.2. Introduction:

Oligomers formed in the initial self-assembly process of $A\beta_{1-42}$ peptide are reported to be the toxic agent [110-112]. While there has been an increasing number of studies carried out to understand the oligomeric structures of $A\beta_{1-42}$ peptide, [117, 118] a conclusive X-ray diffraction or 3-D NMR structure of an $A\beta_{1-42}$ peptide oligomer is yet to be determined [117]. Without atomic level resolution of oligomer structure, the designing of the inhibitors targeting the oligomers remains a challenge. Although

conformational studies on $A\beta_{1-42}$ peptide oligomers have been carried out, limited information is known about the initial stages of oligomerization. In this work, we have investigated the conformational dynamics of the trimer and tetramer of $A\beta_{1-42}$ peptide using MD simulation and analyzed the corresponding MD trajectories to examine their interaction profile. We prepared the initial $A\beta_{1-42}$ trimer and tetramer structures in the M-ZDOCK server [217] using the NMR structure of $A\beta_{1-42}$ from Protein Data Bank. Moreover, using PDBsum server [180], we have investigated the interface statistics and interface residues of the $A\beta_{1-42}$ peptide oligomers. The scoring function used by M-ZDOCK server takes into account the surface complementarity, electrostatics and desolvation to find the optimal fit between two proteins. Surface complementarity is calculated using pairwise shape complementarity (PSC), which consists of a favorable term determined by the number of atom pairs within a distance cutoff, and a penalty term determined by the number of clashes. Atomic Contact Energy (ACE) is used to score desolvation, and the electrostatic term is calculated by applying Coulomb's equation to the partial charges of the ligand in the electrostatic field of the receptor. The search strategy of M-ZDOCK is to discretize both ligand and receptor onto a grid, and use Fast Fourier Transform (FFT) to determine the best position of the ligand relative to the receptor. This discretization and FFT is performed for a complete set of angular orientations of the ligand (relative to a fixed receptor). Results have demonstrated that this approach performs well against a docking benchmark.

One of the interesting features of amyloid formation is that amyloid fibrils display polymorphism at the structural level. Similarly, $A\beta_{1-42}$ peptide can lead to the formation of different molecular structures of $A\beta_{1-42}$ fibrils depending on specific growth conditions [135]. Certain nucleation event and critical nuclei may lead to molecular-level polymorphism of $A\beta_{1-42}$ fibrils [137]. Many experimental studies have tried to identify the polymorphism of $A\beta_{1-42}$ fibrils [132] and the variations in molecular structures underlying the amyloid polymorphism. Here, we have discussed a general structural model of $A\beta_{1-42}$ fibril and different interactions that are responsible for stabilizing the fibril structure as a whole. In this context, we have carried out interaction studies on different dimer models of $A\beta_{1-42}$ fibrils. We have taken the PDB structures of the $A\beta_{1-42}$ fibrils from the protein data bank [212] and constructed the dimer model. The $A\beta_{1-42}$ fibrils that were subjected to study are: $A\beta_{17-42}$ (PDB ID: 2BEG) [125], $A\beta_{MO11-42}$

(PDB ID: 5KK3) [218], $A\beta_{11-42}$ (PDB ID: 2MXU) [219] and full length $A\beta_{1-42}$ (PDB ID: 2NAO) [220] in a different backbone orientation.

8.3. Materials & Methods:

8.3.1. Preparation of initial monomer structure to construct $A\beta_{1-42}$ peptide oligomers:

The initial monomer structure of $A\beta_{1-42}$ peptide was retrieved from Protein Data Bank (PDB) entry: 1IYT [211]. The monomeric structure was then solvated with TIP3P water model with the solvent buffer of 10 Å in all directions [170]. To neutralize the negative charge of the monomer, appropriate numbers of sodium ions were added. Further minimization, heating, and equilibration were carried out as described in Chapter 5 (section 5.3.1.).

8.3.2. Construction of $A\beta_{1-42}$ peptide oligomer structures:

The equilibrated monomer was submitted to M-ZDOCK server to construct the model trimer and tetramer structures. The top scoring trimer and tetramer complexes were selected and then solvated in TIP3P water model and then subjected to a two-step restrained minimization followed by heating. The complexes were then equilibrated for 100 ps followed by MD simulation of 50 ns. Such time was sufficient to obtain a stable configuration. Clustering was performed on a series of MD trajectories [204]. Trajectories were created from the independent runs leading to a partitioning into six clusters. After the MD run, the VMD package [192] was used for visualization of the 3-D structure of the molecule.

8.3.3. Investigation of interface statistics and interface residues in trimer and tetramer of $A\beta_{1-42}$ peptide:

In order to investigate the interface statistics and interface residues of $A\beta_{1-42}$ peptide oligomers, we have submitted the conformer representing the most populated clusters from the MD trajectories in PDBsum server [180] and carried out their interaction studies.

8.3.4. Interaction study of $A\beta_{1-42}$ fibril polymorphs:

The $A\beta_{1-42}$ fibril structures were identified and retrieved from Protein Data Bank and dimer models were constructed. Individual dimer models were then subjected to interaction studies using PDBsum server [180].

8.4. Results & Discussions:

8.4.1. Conformational dynamics of $A\beta_{1-42}$ peptide oligomers:

The initial trimer and tetramer structure of $A\beta_{1-42}$ peptide generated from the M-ZDOCK server are shown in **Figure 8.1**. Individual monomeric chains are marked with different colors and labelled as chain A, B, C and D, respectively.

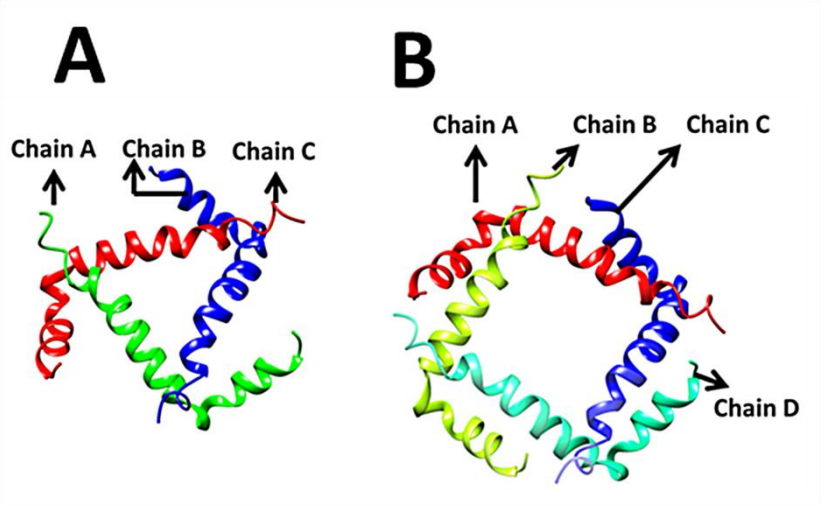

Figure 8.1. *Initial structures generated from the M-ZDOCK server: A) $A\beta_{1-42}$ trimer; B) $A\beta_{1-42}$ tetramer.*

The conformational dynamics of $A\beta_{1-42}$ trimer obtained from MD simulation at different time intervals is illustrated in **Figure 8.2.** From the conformational changes underwent by the dimer complex in 50 ns, we can observe that individual monomeric units undergo slow transition from the α-helical structure to random coils. Since all the three monomeric units are held together very closely, their secondary structural changes over the simulation time period is not drastic. By using the DSSP tool [183] which determines the existence of hydrogen bonds as criteria for the presence of secondary structure, we also examined the secondary structures of $A\beta_{1-42}$ trimer during the course of the simulation. The evolution of the secondary structures from the trajectories as a function of time is shown in **Figure 8.3.** We observed appearance of β-strands at C-terminal regions in the chain C which is encircled in blue.

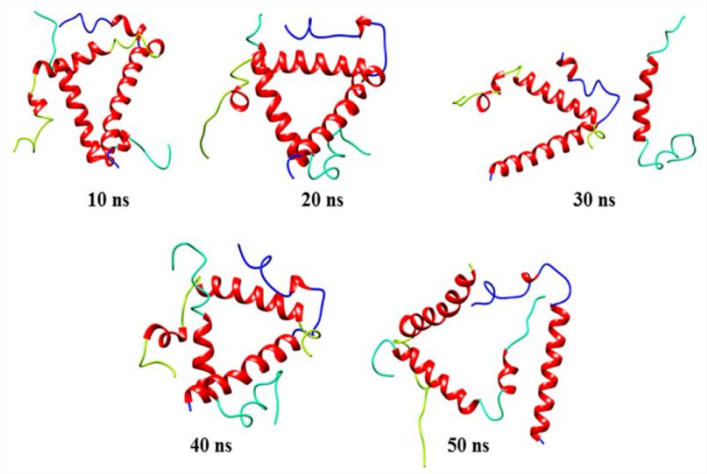

Figure 8.2. *Snapshots of $A\beta_{1-42}$ trimer at different time intervals of simulation.*

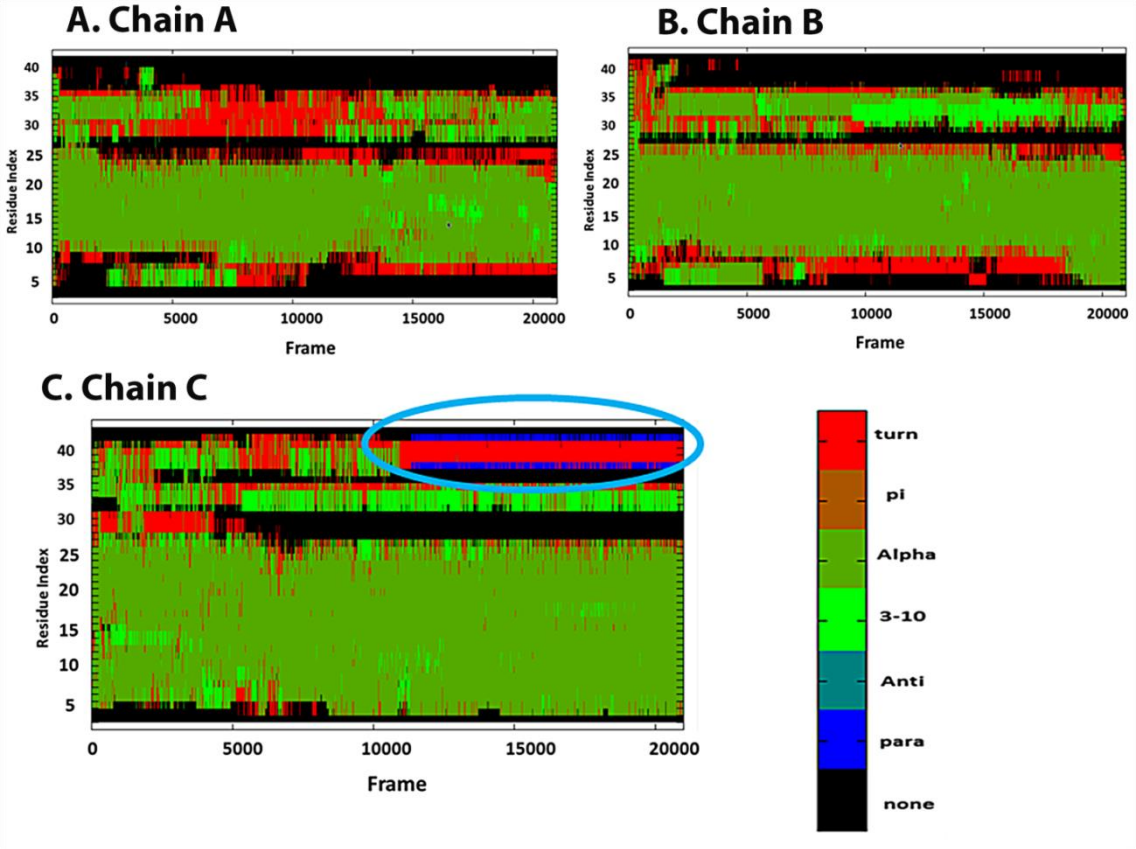

Figure 8.3. *Time evolution of secondary structure of $A\beta_{1-42}$ trimer at 300 K. A)chain A; B) chain B; C) chain C. The encircled area in blue shows the appearance of β-strands.*

Similarly, the conformations of $A\beta_{1-42}$ tetramers at different time interval during the time course of simulation up to 50 ns are shown in **Figure 8.4.** In the case of $A\beta_{1-42}$ tetramer, we can observe the drastic secondary structural changes from the α-helical structure to random coils which may further get converted to β-strands. This is in good agreement with the evolution of the secondary structural analysis (**Figure 8.5**). We observed the appearance of β-strands at C-terminal regions in the chain D.

Additionally, we have compared the secondary structural contents of the initial structure and the average structure of the $A\beta_{1-42}$ trimer and tetramer using YASARA [221]. From **Table 8.1** that provides in detail the secondary structural content, we can see that the initial structures of $A\beta_{1-42}$ trimer and tetramer are rich in helical content ~70%. During the time course of the simulation, all the oligomer complexes underwent secondary structural changes and with the average of structural compositions rich in coils and turns. The helical contents that were predominant in the initial structures declined and the β-sheet content that was 0 % in the initial structure of $A\beta_{1-42}$ peptide oligomers were found to increase. Thus, we can say that the oligomers present in a random coil and turn state have the tendency to acquire β-strands later.

Table 8.1: *Secondary structural analysis of $A\beta_{1-42}$ peptide oligomers.*

Secondary Structures	**$A\beta_{1-42}$ Trimer**		**$A\beta_{1-42}$ Tetramer**	
	Initial Structure	**Equilibrated Structure**	**Initial Structure**	**Equilibrated Structure**
Helix	78.6%	49.2%	67.4%	19%
Sheet	0%	3.2%	0%	11%
Turn	0%	12.7%	5.4%	32%
Coil	21.4%	28.6%	24.5%	38%
3_{-10} helix	0%	6.3%	2.7%	0%

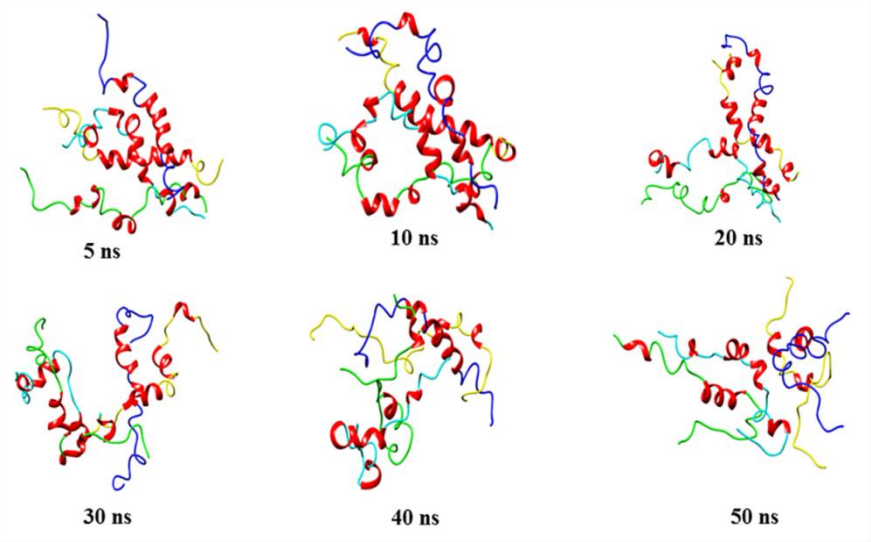

Figure 8.4. *Snapshots of $A\beta_{1-42}$ tetramer at different time intervals of simulation.*

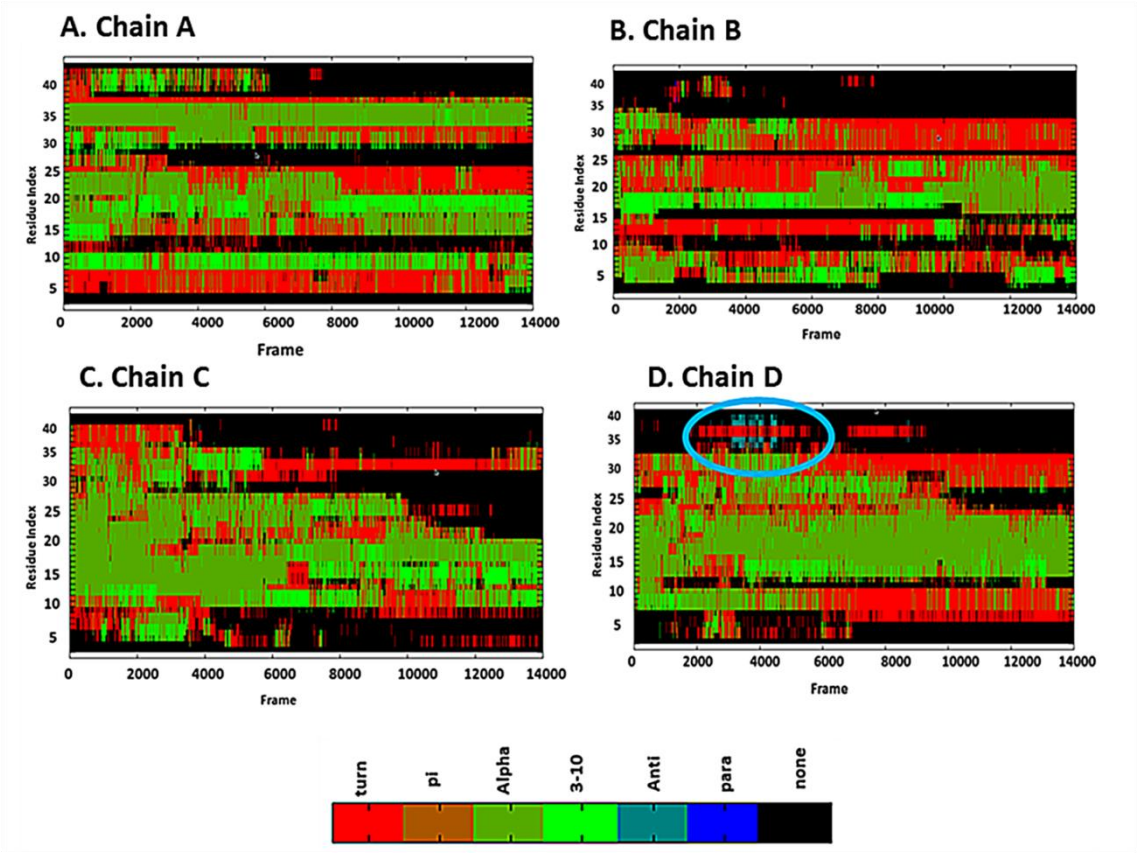

Figure 8.5. *Time evolution of secondary structure of $A\beta_{1-42}$ tetramer at 300 K. A)chain A; B) chain B; C) chain C; D) chain D. The encircled area in blue shows the appearance of β-strands.*

8.4.2. Hydrogen bonding and Hydrophobic contact analysis of $A\beta_{1-42}$ peptide oligomers:

We have calculated the total number of inter-molecular hydrogen bonds and hydrophobic contacts of the $A\beta_{1-42}$ trimer and tetramer that play a vital role in stabilizing the oligomer structures. To calculate the hydrogen bonds, the cut off for angle and distance was set to 120^0 and 3.5 Å respectively. **Figure 8.6** shows the total number of inter-molecular hydrogen bonds between the monomers of $A\beta_{1-42}$ trimer. From **Figure 8.6** we notice ~5 inter-molecular hydrogen bonds to stabilize the interaction between monomer 1 and 2 and ~2 inter-molecular hydrogen bonds to stabilize the interaction of monomer 3 with monomer 1 and 2. We have further shown the acceptor and donor residues that were involved in the formation of the respective hydrogen-bonds in $A\beta_{1-42}$ trimer (**Table 8.2**).

Table 8.2: *Inter-molecular hydrogen bonding analysis of $A\beta_{1-42}$ trimer.*

A. Aβ Monomer 1 (Acceptor): Aβ Monomer 2 (Donor)

A.

Acceptor	Donor	Fraction
ARG_5	GLU_64	0.2210
HIE_13	LEU_59	0.0986
ARG_5	GLU_64	0.0784
HIE_6	VAL_60	0.0775
HIE_6	GLU_64	0.697

B. Aβ Monomer 1 (Acceptor): Aβ Monomer 3 (Donor)

B.

Acceptor	Donor	Fraction
VAL_36	GLU_99	0.3758
GLY_37	GLU_99	0.3600
LYS_28	ASP_91	0.0500
ALA21_6	GLY93_60	0.0441
MET_35	GLU_99	0.0429

C. Aβ Monomer 2 (Acceptor): Aβ Monomer 3 (Donor)

Acceptor	Donor	Fraction
GLU_64	ARG_89	0.3210
PHE_63	LYS_101	0.2986
PHE_62	ARG_89	0.1784
ILE_74	LEU_100	0.0775
GLY_76	GLY_136	0.0697

We have also calculated the total number of hydrophobic contacts between the monomeric units of Aβ$_{1-42}$ trimer from the MD trajectories generated after 50 ns. From **Figure 8.7** we notice monomeric units 1 and 2 to form highest number of hydrophobic contacts ~65. Monomer 1 and 3 formed ~50 numbers of hydrophobic contacts and least number was formed between monomer 2 and 3 ~40.

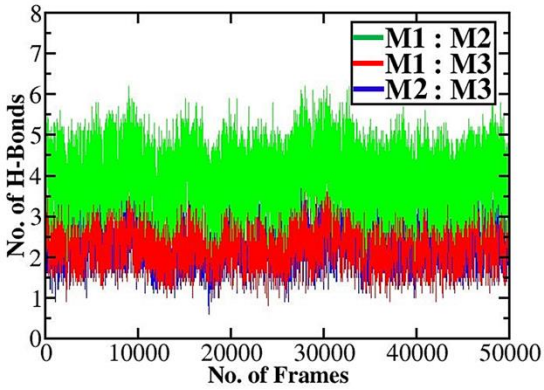

Figure 8.6. *Total number of inter-molecular hydrogen bonds vs total number of frames for the Aβ$_{1-42}$ trimer during the time course of simulation at 300 K.*

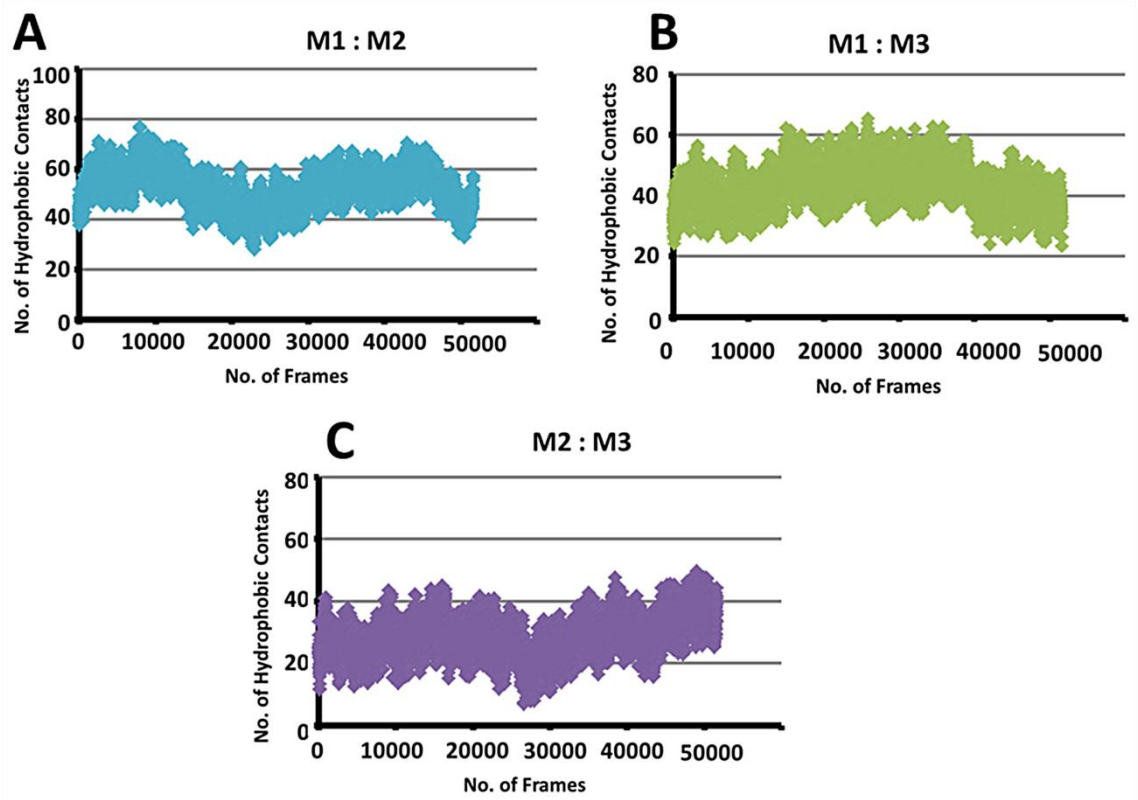

Figure 8.7. *Total number of hydrophobic contacts vs total number of frames for the Aβ$_{1-42}$ trimer during the time course of simulation at 300 K.*

Likewise, the total numbers of inter-molecular hydrogen bonds between the monomers of $A\beta_{1-42}$ tetramer are illustrated in **Figure 8.8**. From **Figure 8.8.A,** we observed monomer 1 to form ~6 and 3 inter-molecular hydrogen bonds with monomer 2 and monomer 4, respectively. Monomer 3 was found to form 3 inter-molecular hydrogen bonds with monomers 2 and 4 (**Figure 8.8.B**). We have further shown the acceptor and donor residues that were involved in the formation of the respective hydrogen-bonds in $A\beta_{1-42}$ tetramer (**Table 8.3**). The hydrophobic contacts between different monomeric units in tetramer are shown in **Figure 8.9**.

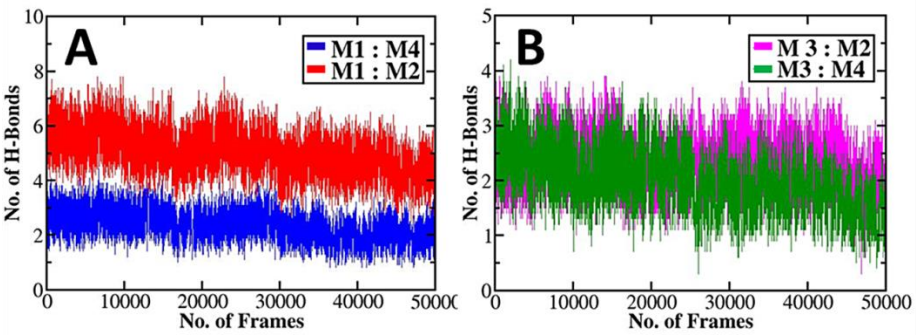

Figure 8.8. *Total number of inter-molecular hydrogen bonds vs total number of frames for the $A\beta_{1-42}$ tetramer during the time course of simulation at 300 K.*

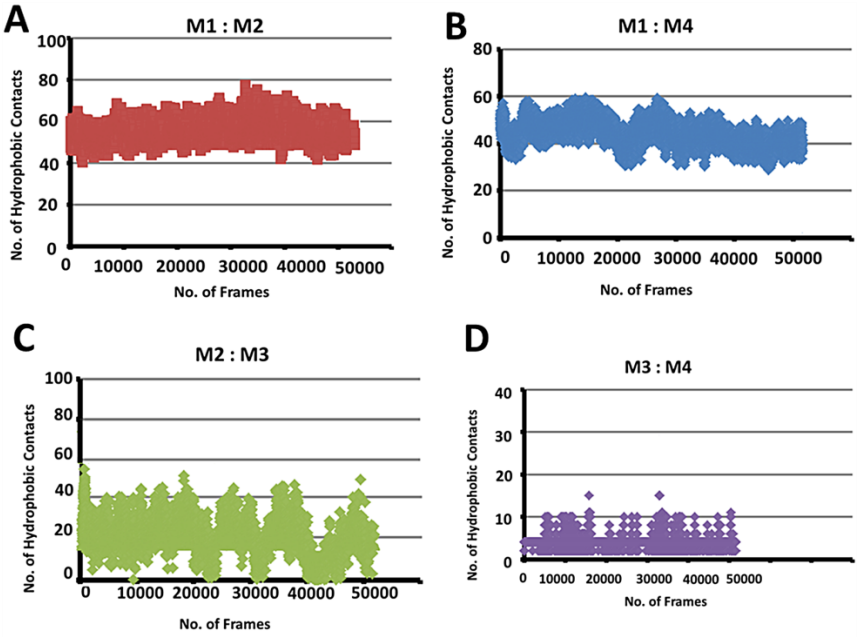

Figure 8.9. *Total number of hydrophobic contacts vs total number of frames for the $A\beta_{1-42}$ trimer during the time course of simulation at 300 K.*

***Table 8.3**: Inter-molecular hydrogen bonding analysis of $A\beta_{1-42}$ tetramer.*

A. Aβ Monomer 1 (Acceptor): Aβ Monomer 2 (Donor)

Acceptor	Donor	Fraction
ARG_5	ASP_49	0.3991
SER_8	SER_50	0.1677
HIE_13	GLU_64	0.1425
ARG_5	GLU_53	0.0954
LYS_16	ASP_65	0.0864

B. Aβ Monomer 1 (Acceptor): Aβ Monomer 3 (Donor)

Acceptor	Donor	Fraction
SER_8	VAL_96	0.0029
SER_8	HIE_97	0.0020
GLY_9	HIE_97	0.0005
LEU_34	ASN_111	0.0003
VAL_12	HIE_97	0.0003

C. Aβ Monomer 1 (Acceptor): Aβ Monomer 4 (Donor)

Acceptor	Donor	Fraction
LYS_16	ASP_149	0.0514
ILE_41	LYS_154	0.0500
HIE_14	ARG_131	0.0157
HIE_13	ARG_149	0.0032
HIE_13	ASP_127	0.0032

D. Aβ Monomer 2 (Acceptor): Aβ Monomer 3 (Donor)

Acceptor	Donor	Fraction
ARG_47	ASP_91	0.5271
HIE_48	GLU_95	0.4387
TYR_52	GLU_106	0.2635
HIE_55	ASP_107	0.1126
LYS_58	HIE_97	0.1101

E. Aβ Monomer 2 (Acceptor): Aβ Monomer 4 (Donor)

Acceptor	Donor	Fraction
ASP_49	ASP_133	0.1054
SER_50	SER_134	0.0910
HIE_48	GLU_129	0.0900
GLU_53	SER_134	0.0874
ASP_65	GLU_137	0.0638

F. Aβ Monomer 3 (Acceptor): Aβ Monomer 4 (Donor)

Acceptor	Donor	Fraction
MET_77	MET_152	0.1130
MET_77	GLY_157	0.1021
LEU_76	GLU_129	0.0865
VAL_78	SER_134	0.0844
LEU_76	GLU_137	0.0638

8.4.3. Interface statistics and residue-residue interaction study of $A\beta_{1-42}$ peptide oligomers using PDBsum server:

Additionally using PDBsum server [180], we have investigated the interface statistics and the residues involved in the formation of the $A\beta_{1-42}$ peptide oligomers. The interface statistics of the $A\beta_{1-42}$ trimer is provided in **Table 8.4.** As shown in **Table 8.4**, a large number of non-bonded contacts, seven hydrogen bonds, and three salt bridges were found to aid in the association of monomeric units to form a stabilized trimer structure. The interface area was found to be highest between chains A and B which is ~700 $Å^2$. Furthermore, we have highlighted the residues involved in the formation of the inter-peptide salt bridges of the monomeric units of $A\beta_{1-42}$ trimer in **Table 8.5.**

Likewise, we carried out the protein-protein interaction studies in the PDBsum server for the full length $A\beta_{1-42}$ tetramer structure. Different interactions that play a crucial role in the tetramer formation are shown in **Table 8.6**. Six inter-peptide salt bridges were found to stabilize tetramer structure. A total of sixteen inter-molecular hydrogen bonds and a large number of non-bonded contacts were found to stabilize the tetramer structure. Furthermore, we have highlighted the residues involved in the formation of the inter-peptide salt bridges of the monomeric units of $A\beta_{1-42}$ tetramer as shown in **Table 8.7**.

Table 8.4: *The interface plot statistics of the $A\beta_{1-42}$ trimer as predicted by the PDBsum server.*

Chain	No. of Interface Residues	Interface Area (Å^2)	No. of Salt Bridges	No. of Hydrogen Bonds	No. of Non-bonded Contacts
A : B	12 : 12	733 : 668	2	4	63
A : C	9 : 9	609 : 590	0	2	40
B : C	8 : 8	418 : 411	1	1	35

Table 8.5: *The inter-peptide salt bridge analysis of the $A\beta_{1-42}$ trimer as predicted by the PDBsum server.*

Chain	Atom No.	Residue name	Atom name	Residue No.		Atom No.	Residue name	Atom name	Residue No.
A : B	79	ARG	NH2	5	↔	981	GLU	OE2	64
A : B	163	GLU	OE1	11	↔	1060	LYS	NZ	70
B : C	640	ASP	OD2	43	↔	1688	LYS	NZ	112

Table 8.6: *The interface plot statistics of the $A\beta_{1-42}$ tetramer as predicted by the PDBsum server.*

Chain	No. of Interface Residues	Interface Area (Å^2)	No. of Salt Bridges	No. of Hydrogen Bonds	No. of Non-bonded Contacts
A : B	7 : 11	533 : 496	3	6	55
A : D	8 : 8	442 : 447	1	3	43
B : C	5 : 6	345 : 347	1	4	33
B : D	1 : 1	73 : 74	0	0	4
C : D	5 : 5	319 : 356	1	3	39

Table 8.7: *The inter-peptide salt bridge analysis of the $A\beta_{1-42}$ tetramer as predicted by the PDBsum server.*

Chain	Atom No.	Residue name	Atom name	Residue No.		Atom No.	Residue name	Atom name	Residue No.
A : B	73	ARG	NE	5	↔	980	GLU	OE1	64
A : B	79	ARG	NH2	5	↔	981	GLU	OE2	64
A : B	163	GLU	NZ	11	↔	1060	LYS	NZ	70
A : B	627	ALA	OXT	42	↔	707	ARG	NH2	47
A : C	536	VAL	N	36	↔	1484	GLN	OE1	99
A : C	552	GLY	N	37	↔	1484	GLN	OE1	99
B : C	723	HIE	NE2	48	↔	1609	GLU	OE2	106

Additionally, we have carried out salt-bridge analysis from the MD trajectories to assess the relevance of the PDBsum data by measuring the distance between the center of mass of the residues that formed the salt-bridges in trimer and tetramer. Salt bridge that normally exists in $A\beta_{1-42}$ peptide has been reported to play an important role in stabilizing the peptide structure. From **Figure 8.10,** we can see that the distance between the center of mass of the residues to be less than 5 Å at certain time period of simulation, which validated the salt bridge. Thus the salt-bridges that were reported to be formed between the monomeric units in the trimer and tetramer complexes by PDBsum server were found to be valid and thus they might play an important role in stabilizing the oligomers.

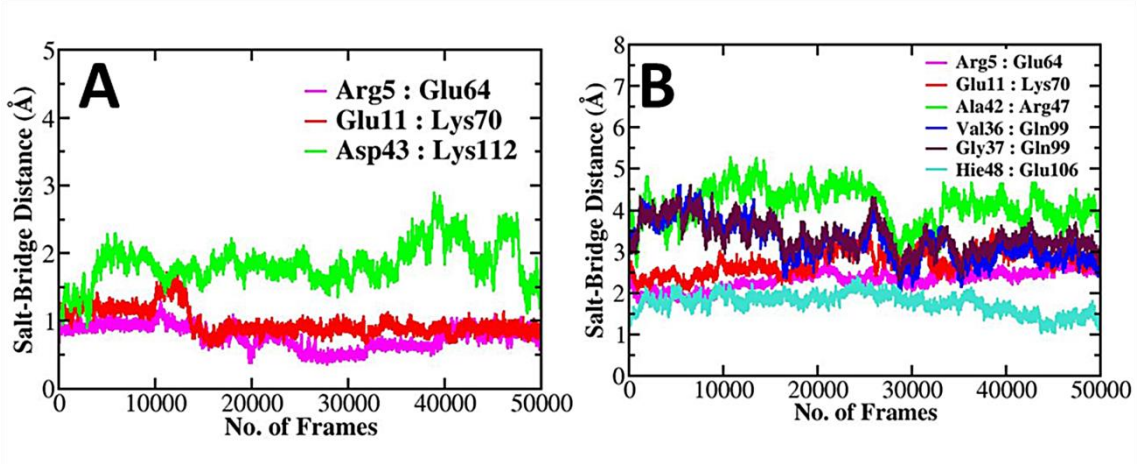

Figure 8.10. *Inter-peptide salt-bridge vs total number of frames for A) $A\beta_{1-42}$ trimer; B) $A\beta_{1-42}$ tetramer during the time course of simulation at 300 K.*

8.4.4. Structural characterization of polymorphic $A\beta_{1-42}$ fibrils:

A primary property of amyloid fibrils is their ability to proliferate by addition of misfolded monomers from their surroundings. Likewise, polymorphism is another important property of amyloid fibrils. Amyloid fibril polymorphs are the variety of bundled arrangements of the basic amyloid protofilament structures [222]. These polymorphs contain distinct molecular structures and thus can propagate themselves [223].

In this study, we have examined the structural variations of $A\beta_{1-42}$ fibril polymorphs that are reported in the Protein Data Bank. **Figure 8.11** illustrates the PDB structures of four polymorphs of $A\beta_{1-42}$ fibril. From **Figure 8.11.A**, which shows the 3-D Aβ fibril structure encompassing residues 17–42, we can see that the fibril consists of two intermolecular, parallel, in-register parallel β-sheets that are formed by residues

encompassing regions 18–26 and 31–42 with one U-turn. Asp23 and Lys28 were found to form a salt bridge. The residues Phe19 and Gly38 appeared to form a hydrophobic interaction pair that connects the two β-strands.

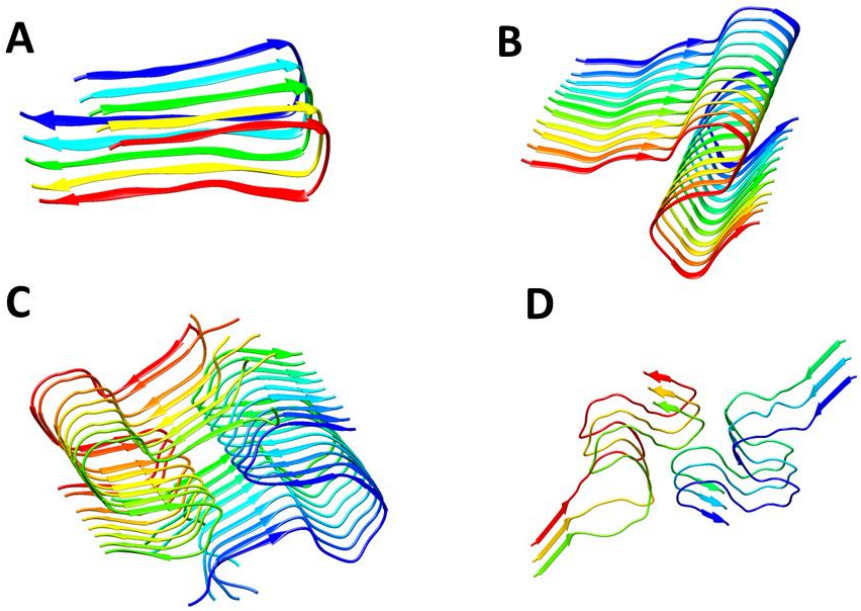

Figure 8.11. *Snapshots of $A\beta_{1\text{-}42}$ fibril polymorphs: A) $A\beta_{17\text{-}42}$; B) $A\beta_{11\text{-}42}$; C) $A\beta_{MO11\text{-}42}$; D) $A\beta_{1\text{-}42}$.*

Similarly, a solid-state 3-D NMR model of $A\beta_{1\text{-}42}$ fibril structure encompassing residues 11-42 was obtained from the Protein Data Bank (**Figure 8.11.B)**. The structural features of the $A\beta_{11\text{-}42}$ fibril provide insight into how tertiary folds of amyloid proteins can be different by adopting alternative states. $A\beta_{11\text{-}42}$ fibril forms S-shaped triple parallel β-sheet structure. Salt bridge between Lys28 and Ala42 was formed via an intra-molecular contact. Likewise, a monomorphic form of $A\beta_{MO11\text{-}42}$ fibril obtained from high field magic angle spinning NMR spectra is shown in **Figure 8.11.C**. The fibril structure shows that the $A\beta_{MO11\text{-}42}$ fibril core consists of a dimer containing four β-strands in S-shaped fold generating two distinct hydrophobic cores, one containing residues Ile31, Val36, V39, and Ile41, and the other containing Leu17, Phe19, Phe20, Val24, Ala30, and Ile32. Some of the contacts important for determining the fold of the monomer structure were found to be between Phe19-I32, Phe19-Ala30, Phe20- Val24, Val24-Gly29, Ile31-Val36, Gly33-Val36, Gly29-Ile41, and Lys28- Ala42.

Figure 8.11.D shows a disease-relevant 3-D solid-state NMR structure of $A\beta_{1\text{–}42}$ fibril with in-register parallel intermolecular β-strands that winds up around the two

hydrophobic intra-molecular cores in a double horseshoe-like position. The β-sheet was found to interact through the hydrophobic side chains. This hydrophobic core was complemented by an asparagine ladder with the side chain of Asn27 and a glutamine ladder involving the side chain of Glu15. Both Phe19 and Phe20 faced towards the hydrophobic core requiring a special non–β-strand-like backbone conformation. While subtle differences among these models exist, some features are common among the models. From our study, we found the presence of turn and extended β-strands in the residues 11-42 to be present in all the polymorphs.

8.4.5. Interaction studies of polymorphic $A\beta_{1-42}$ fibrils:

In order to understand the mechanism by which individual monomeric units interact with each other to form a stable fibril structure, we examined their inter-molecular interactions. We modelled the dimer structure of each polymorph and carried out their interaction studies in PDBsum server.

i. **$A\beta_{17-42}$ Dimer Interaction Study:** The highly amyloidogenic central hydrophobic region of Aβ peptide, which includes the residues from 17-42 has provided a prototype for the assembly of Aβ peptide in general. We have used $A\beta_{17-42}$ as a dimer model to explore the interactions as illustrated in **Figure 8.12. Figure 8.12** displays the residues interacting through non-bonded contacts, salt-bridges and hydrogen bonds, and the interface statistics obtained from the PDBsum server. From **Figure 8.12** we found 1 salt bridge, 24 inter-molecular hydrogen bonds and a lot of (231) non-bonded contacts to stabilize the dimer.

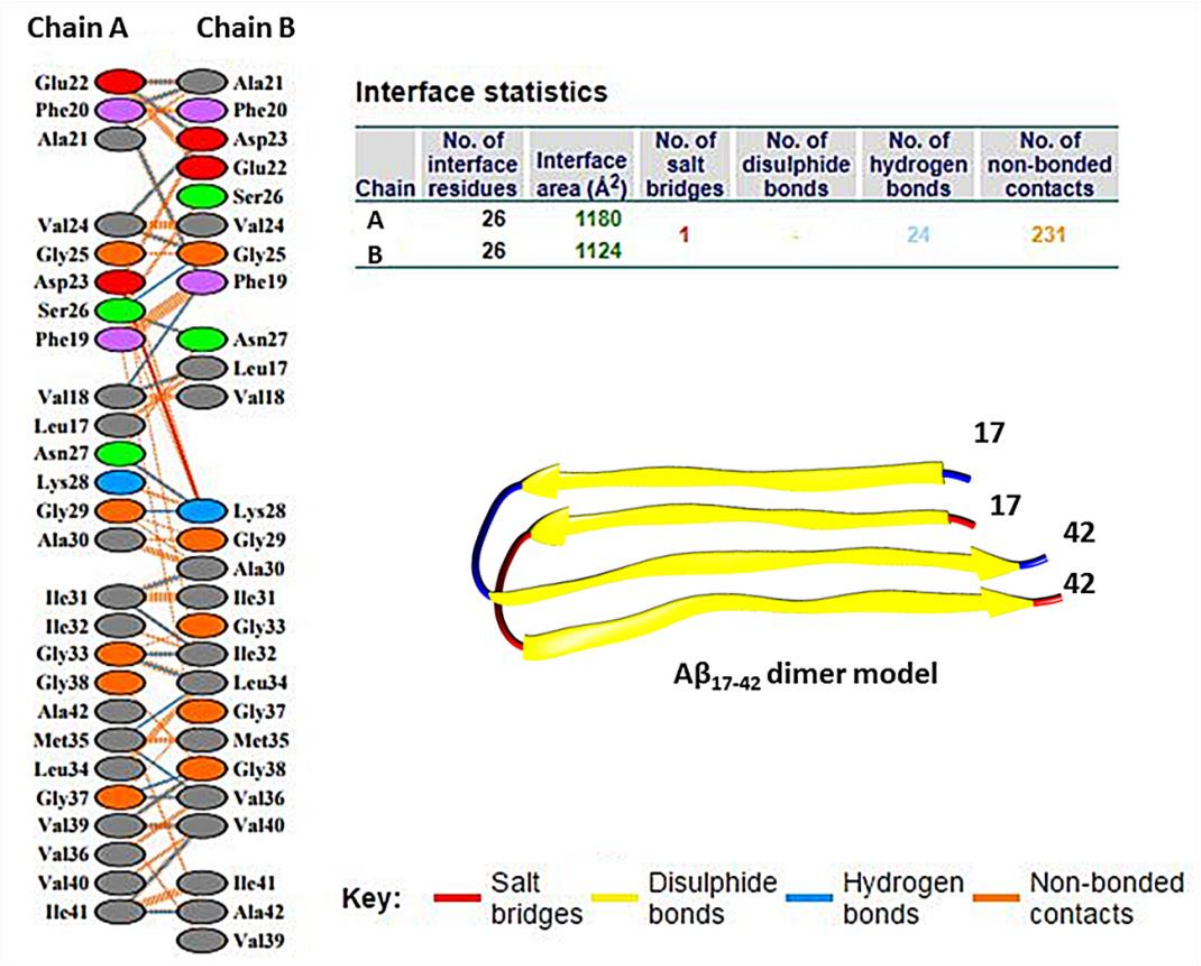

Figure 8.12. *The interface residues and interface plot statistics in $A\beta_{17-42}$ dimer as predicted by PDBsum server.*

ii. $A\beta_{11-42}$ Dimer Interaction Study:

N-terminal truncated $A\beta_{11-42}$ found in the cerebrospinal fluid has been reported to constitute one fifth of the senile plaques [224]. In light of its vital role in amyloid formation, we studied the interaction profile of this fragment. **Figure 8.13** shows the residues involved in various interactions like salt-bridges, inter-molecular hydrogen bonds and non-bonded contacts in stabilizing the $A\beta_{11-42}$ dimer model. We can see that, similar to $A\beta_{17-42}$ dimer model, $A\beta_{11-42}$ also forms 1 salt-bridge, 31 hydrogen bonds and a lot of (190) non-bonded contacts.

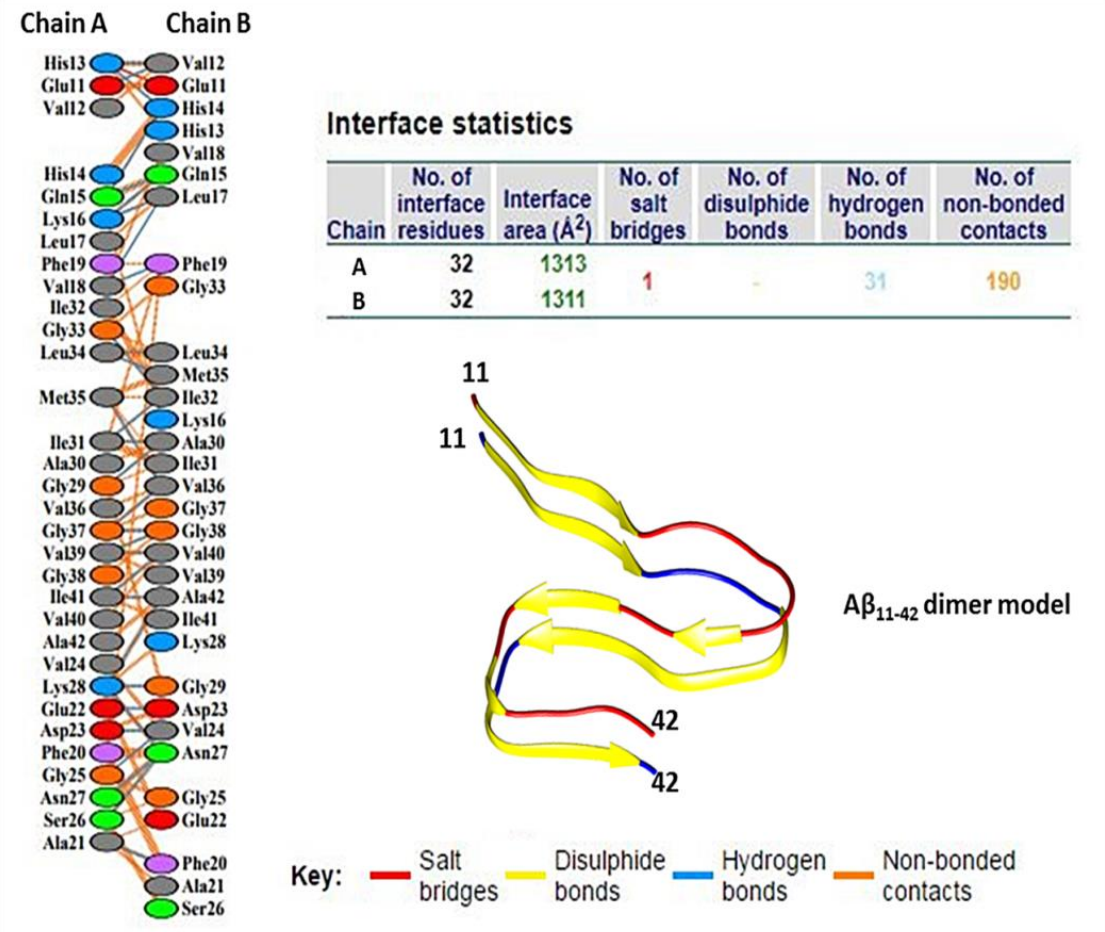

Figure 8.13. *The interface residues and interface plot statistics in $A\beta_{11-42}$ dimer as predicted by PDBsum server.*

iii. **$A\beta_{MO11-42}$ Dimer Interaction Study:** Here, we used monomorphic form of $A\beta_{M01-42}$ amyloid fibril to construct the $A\beta_{MO1-42}$ dimer model with four β-strands in an S-shaped amyloid fold. The interaction result for $A\beta_{MO11-42}$ dimer is illustrated in **Figure 8.14. Figure 8.14** displays the residues interacting through non-bonded contacts and hydrogen bonds, obtained from the PDBsum server. Leu17, Leu34, Met35 and Val 36 that formed non-bonded contacts were hydrophobic in nature. Gln15 of Chain A formed a hydrogen bond with Val36 of Chain B.

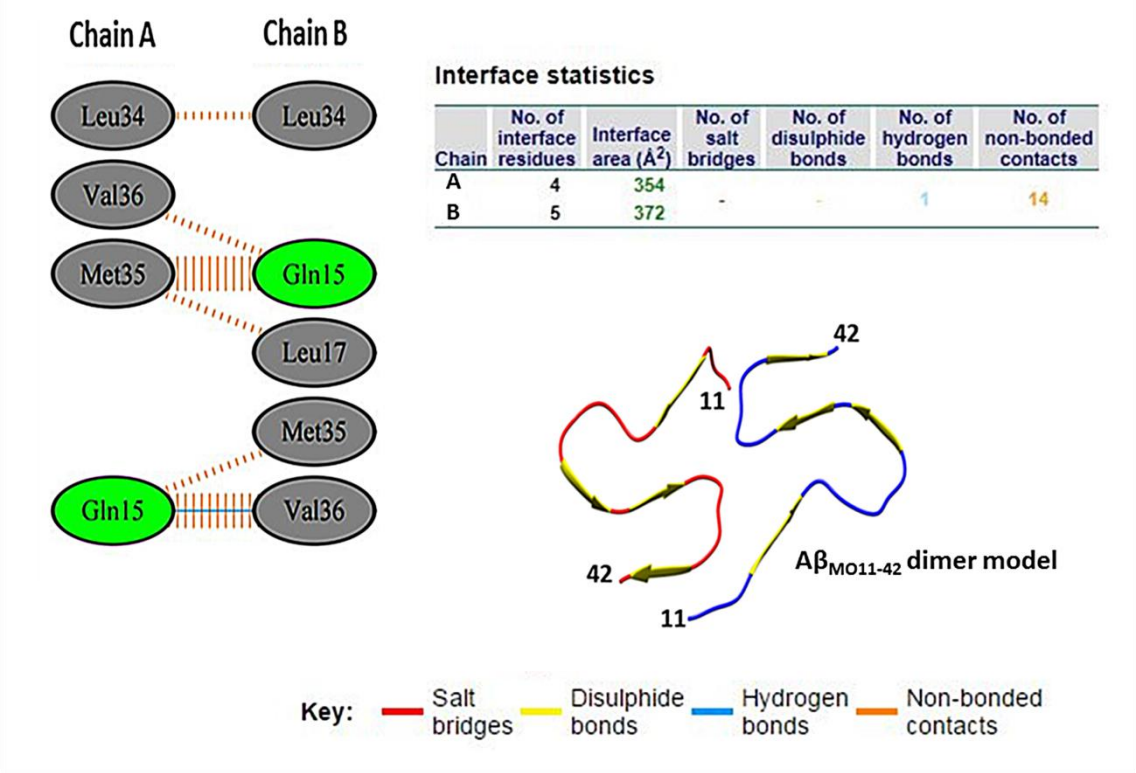

Figure 8.14. *The interface residues and interface plot statistics in $A\beta_{MO11-42}$ dimer as predicted by PDBsum server.*

iv. **$A\beta_{1-42}$ Dimer Interaction Study:** Fragments can arise because of difference in their backbone orientation. A disease-relevant 3-D solid-state NMR structure of $A\beta_{1-42}$ amyloid fibril with β-strands was used to model the dimer of $A\beta_{1-42}$. Accordingly, we studied the interaction mechanism of the dimer. The interaction result for $A\beta_{1-42}$ dimer is illustrated in **Figure 8.15. Figure 8.15** displays the residues interacting through non-bonded contacts obtained from the PDBsum server. From **Figure 8.15,** we found that most of the residues that formed non-bonded contacts were from the C-terminal regions, and were hydrophobic in nature.

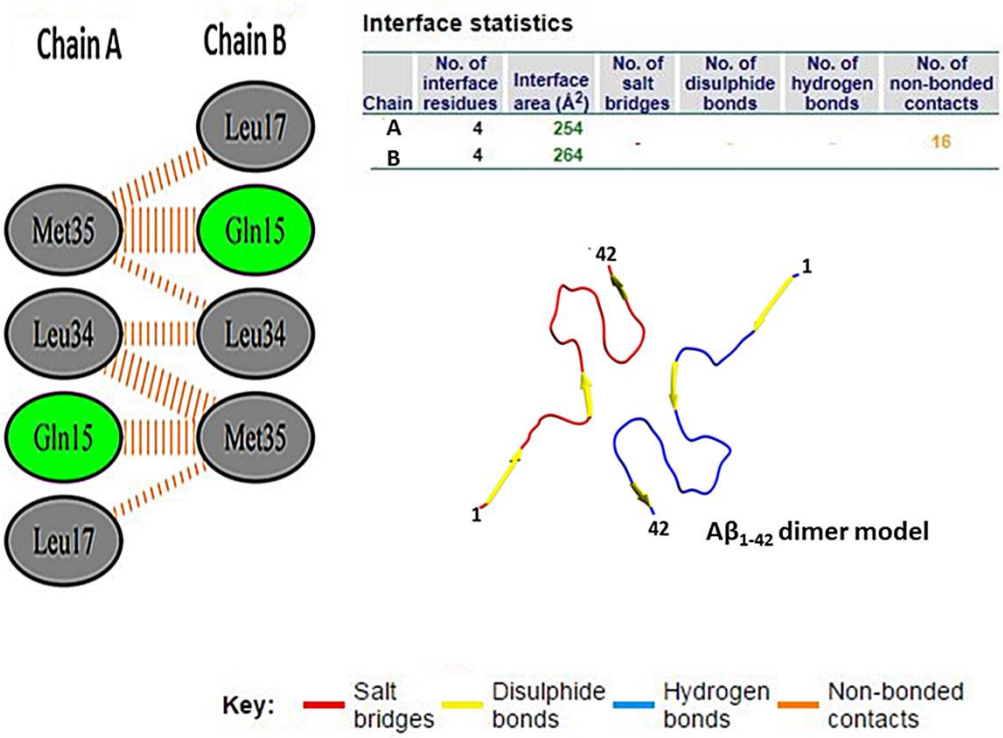

Figure 8.15. *The interface residues and interface plot statistics in $A\beta_{1-42}$ dimer as predicted by PDBsum server*

8.5. Conclusions:

Due to the flexibility and the high susceptibility to undergo aggregation, the low molecular weight, toxic $A\beta_{1-42}$ peptide oligomers are not easy to study. In this work, we have carried out all-atom MD simulation study on full-length $A\beta_{1-42}$ trimer and tetramer, and further studied the interactions that hold together the individual monomeric units. Our results suggest that the formation of a stable $A\beta_{1-42}$ peptide oligomer occurs through secondary structural transitions from α-helix to random coils which may further form β-strands. The conformations observed in our study may represent transient structures that may be formed during the oligomerization of $A\beta_{1-42}$ peptide. From the interaction study, we found the inter-peptide salt bridges, hydrogen bonds and non-bonded contacts to play a crucial role in stabilizing the oligomers.

One of the interesting features of amyloid formation is that amyloid fibrils display polymorphism at the structural level. On the available $A\beta_{1-42}$ fibril structures in Protein Data Bank, we examined their structural variations and carried out interaction studies using the PDBsum server. Our results suggested the presence of turn and extended β-stranded secondary structures to be predominant in the region encompassing residues 11-42 of $A\beta_{1-42}$ fibril in all the polymorphs. Additionally, CHC region and C-terminal region were found to be involved in the intermolecular interactions in all the polymorphs. This result is consistent with the $A\beta_{17-42}$ peptide dimer interaction results as discussed in Chapter 5. Thus our interaction study proves that CHC region and C-terminal region play an important role in the aggregation of $A\beta_{1-42}$ peptide.